OFFICE FEDERAL DE L'ENERGIE

3003 BERNE

RAPPORT ANNUEL 2002

Pour les travaux de recherche définis dans le projet No 36826

No de contrat 85434

Titre du projet : La photolyse de l'eau et la production d'hydrogène et d'oxygène au moyen de l'énergie solaire

Résumé :

Nos recherches ont été axé plus particulièrement sur :

1) L'élaboration par pyrolyse-spray d'électrodes transparentes et photosensibles en oxyde de fer (αFe_2O_3,hématite). Ces photo-anodes produisent des courants de photo-électrolyse de l'eau de l'ordre de 4 à 6 mA/cm^2. Les améliorations qui ont conduit à ces résultats ont été possibles grâce à la maîtrise des paramètres suivants : température de pyrolyse, refroidissement des échantillons et compréhension des problèmes liés aux différentes qualités de verre conducteur. Des réponses spectrales sont présentées pour les deux types de précurseurs utilisés.

2) L'étude approfondie de la morphologie des films obtenus a été réalisée par spectroscopie Raman et par diffraction de rayons-X.

3) Le développement d'un nouveau concept de 3 électrodes "en ligne" conduisant à une augmentation significative de la quantité de lumière incidente absorbée.

4) La réalisation d'électrodes de tailles nettement supérieures (scaling-up) de 10 cm x 10 cm dans le cadre d'un projet de démonstration.

Durée du projet : 1 an

Mandataire : J. Augustynski
Rapporteurs : C. Jorand Sartoretti, M. Ulmann , B. Alexander
Adresse : Université de Genève
Chimie Minérale, Analytique et Appliquée
Sciences II ; 30 quai E. Ansermet
1211 Genève 4
Téléphone : 022 702 64 13

1-2 Goals, developments and results

I IMPROVEMENTS IN THE PREPARATION OF FERRIC OXIDE, α-FE_2O_3, FILMS.

This report describes new developments in the deposition of iron oxide thin films on conducting glass substrates using the spray-pyrolysis method. These coatings should not only be photoactive, but also transparent in view of their application in a tandem photoelectrolysis cell.

Following our previous experiments, we decided to continue the development using two different precursors in alcoholic solutions:

1) Chloride (type C) : $FeCl_3.6H_2O$

2) Acetylacetonate (type A) : $Fe(acac)_3$

We previously reported that the temperature of spray-pyrolysis for the type C electrodes ranged between 400 to 440 °C. In the case of acetylacetonate, thermal decomposition has been studied by thermogravimetric analysis (TGA) in air, showing that above 365°C, $Fe(acac)_3$ starts to decompose to iron oxide. We deposited the films at 370°C, in the same way as for chloride precursor and then continued the decomposition by raising the temperature of the films up to 550°C for 30 min to 1 hour depending on the number of layers. At the end of the spray-pyrolysis, the samples are cooled under nitrogen atmosphere during 5 to 10 min.

To induce the alpha form during crystallisation of the iron oxide films (α-Fe_2O_3), we tried the addition of (α-Al_2O_3), which is isomorphous to the structure of hematite, into the spraying mixture, but did not obtain any significant improvement in the photocurrents.

Tin has also been tried as doping agent of the iron oxide films (introduced as 1 to 5% $SnCl_2.2H_2O$), but the measured photocurrents were lower than those obtained with titanium dopant. Experiments are currently continuing to determine if a mixture of tin with other doping agents (Ti, Al, ...) could improve the efficiency of the iron oxide films.

IA PHOTOELECTROCHEMICAL RESULTS

UV-visible light

A xenon lamp (150 W, uv-visible wavelengths) has been used to measure the photocurrent-voltage characteristics of iron oxide thin films obtained using both kinds of precursors (type A and C).

The photocurrents listed below have been recorded at a potential of 0.6 V vs. NHE in a 1M sodium hydroxide solution.

The best electrodes of type C without added dopant were obtained for a small number of individual layers, e.g. 3, giving a photocurrent lower than 2 mA/cm^2. The adjunction of titanium(IV), as previously reported, raises the photocurrents up to more than 5 mA/ cm^2. Different mixtures of Ti and Al have been tried showing that the amount of aluminium should not exceed 1% to maintain large photocurrents.

In the case of the precursor A, we observe a different trend. Apparently, dopants play a minor role and the number of applied layers can be much higher without affecting significantly the transparency of the film, which is not the case for the electrodes of type C.

The corresponding photocurrents are comparable with those for the electrodes obtained using the chloride precursor reaching more than 6 mA/cm^2 for the best electrodes.

Precursor	Dopant	Number of layers	Photocurrent measured at 0.6 V vs. NHE (mA/cm^2)
Chloride 42	No	3	1.78
Chloride 46	Ti(1%)	6	5.22
Chloride 141	Ti(5%)	6	5.40
Chloride 166T	Ti(5%)+Al(1%)	6	6.40
Chloride 104	Ti(5%)+Al(5%)	6	3.87
Acetylacetonate 170T	No	15	6.11
Acetylacetonate 177T	No	6	5.07
Acetylacetonate 116T	Ti(5%)	18	6.17
Acetylacetonate 111T	Ti(5%)+Al(5%)	23	4.15

Table 1

Spectral responses

The spectral photoresponses recorded for both kinds of electrodes (obtained using precursors A and C) have a similar shape. An important feature is that for C (chloride) type films, we still observe a photoconversion of 3.7 % at a wavelength of 550 nm and 1.07% at 600 nm In the case of the acetylacetonate precursor, we measured 1.44 % at 550 nm and less than 1 % at 600 nm.

Fig. 1 shows the photocurrent efficiency versus wavelength curves for three films (measured at 0.7 V vs. NHE):

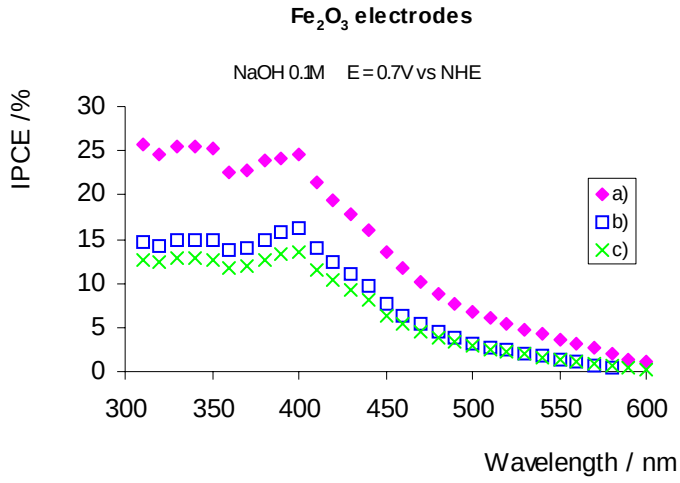

Fig. 1 Incident photon-to-current conversion efficiency (IPCE) % measured at 0.7 V vs. NHE in 0.1M NaOH for a) type C, doped with Ti 5% and Al 1%, 6 layers, b) type A, undoped, 12 layers c) type A, undoped, 6 layers

The quantum yield (IPCE) observed for the films of type A (acetylacetonate precursor) is enhanced with increasing the number of layers, as was previously observed for chloride type films, but it still remains lower than that for the C type films.

Morphological studies

Raman Analysis.

The crystalline composition of the samples can be readily obtained from Raman microscopy measurements. Spectra were recorded using a LabRam I Raman microscope, equipped with a CCD camera, operating in confocal mode, i.e. by closing the confocal pinhole to 200 µm. Employing this size of aperture with a 100 × sampling objective, ensured an estimated sampling depth of 3 µm. The irradiation source was a frequency doubled Nd:YAG laser (532.0 nm) and spectra were recorded from a number of positions on the surface and were found to be highly reproducible. Figure 2 details the Raman spectra obtained for thin films prepared by the spray-pyrolysis from different precursors. These spectra are typical of those obtained from thin films formed with each of the given precursors.

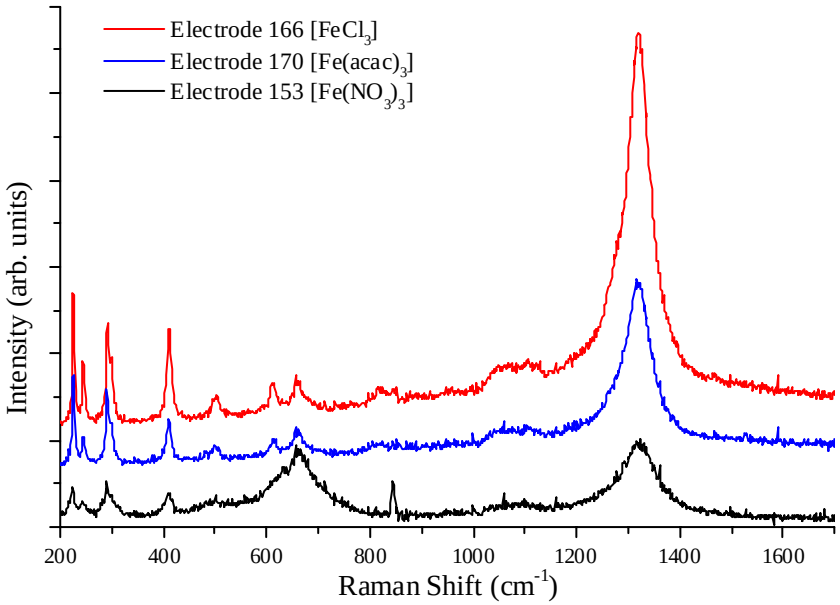

Fig. 2. Raman spectra of thin films of iron oxide prepared using different precursors.

Comparison with both our library spectra of pure iron oxide powders and literature data for iron oxide minerals[1] shows that the bands within the 200-625 cm^{-1} region can be readily assigned to hematite, α-Fe_2O_3. The strong broad band centred *ca.* 1320 cm^{-1} is considered to arise from second order magnon resonance Raman scattering[2] and is present in the spectra of both our pure powders and of natural hematite minerals.

Table 2. Typical sample Raman peaks compared to minerals and powders.

Sample	Band positions (cm^{-1})									
Electrode 166	225.0	244.3	292.3	411.1	503.4		610.0	660.6		1321.0
Electrode 170	226.6	244.3	290.7	409.6	500.3		611.6	662.1		1316.8
Electrode 153	225.0	244.3	290.7	411.1	500.3		616.2	662.1		1321.0
Hematite (powder)	223.5	242.8	289.2	408.1	497.3		610.1			
Magnetite (powder)						540.7		665.2		
Maghemite (powder)								666.7	718.4	
Hematite (mineral)[1]	226.7	245.7	292.5	410.9	497.1		611.9			1322
Magnetite (mineral)[1]						533.6		662.7		
Wüstite (mineral)[1]								652.0		

As can be observed from table 2, most of the bands that appear in the spectra can be assigned to hematite phonons with the exception of the band at *ca*. 660 cm^{-1}. Upon comparison with the Raman spectra of our powders (figure 3) and literature[1], this band can confidently assigned to magnetite, Fe_3O_4. It is possible that this band could be due to other iron oxide species, most likely maghemite, γ-Fe_2O_3, or wüstite, FeO, however, both of these possibilities can be ruled out.

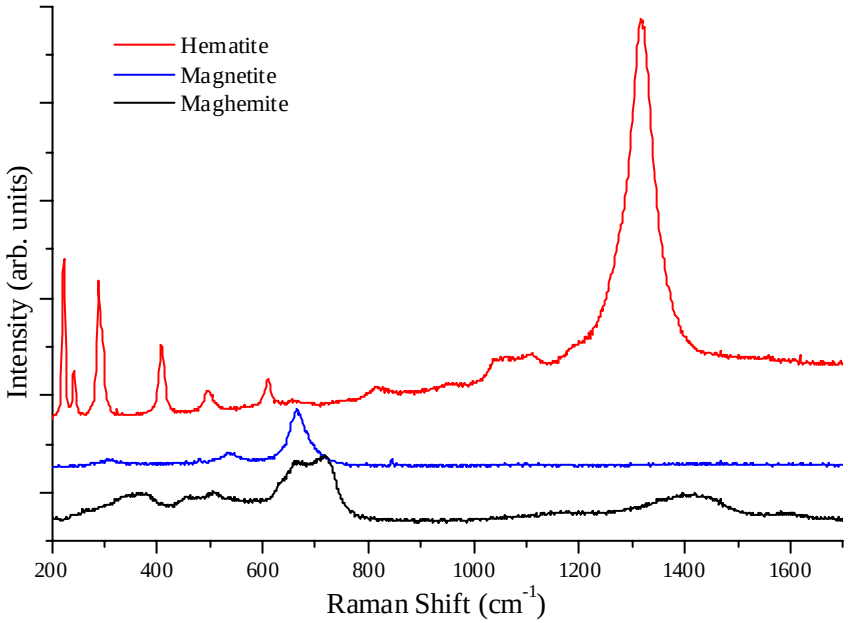

Fig. 3. Sample of library of Raman spectra of iron oxide powders.

As can be seen from figure 3, maghemite presents an unresolved doublet between 650 and 725 cm^{-1}, with the stronger band centred at 718 cm^{-1}. Wüstite has been reported to give a band at 652 cm^{-1}. It is also reported to be thermally unstable[1,3,4] and thus may be unlikely to be present after the film preparation process. However, further investigation is needed to truly discount the presence on wüstite in the iron oxide films. The spectra in figure 2 do not show any evidence of hydrated forms of iron oxide, although this may be due to the relative scattering cross sections when compared to hematite. Determination of the size of the surface features from the low-frequency region is not possible due to the cut-off of the notch filter used. Furthermore, it has already been shown to be impossible to determine the size of Fe_2O_3 nanoparticles from the low-frequency region[5].

The most striking feature of figure 2 is the notable difference in the spectra of the films prepared using $FeCl_3$ and $Fe(acac)_3$ compared to those obtained using $Fe(NO_3)_3$ precursors. It is quite clear that the content of hematite is drastically reduced in the films prepared using $Fe(NO_3)_3$ and that although the spectrum is dominated by the strong second order magnon scattering band of hematite, the magnetite band at 655 cm^{-1} is of equal intensity.

Given that the cross section of the band at 665 cm^{-1} of magnetite is *ca*. 7 times that of the second order magnon band, as shown in figure 3, it follows therefore that there is considerably less hematite present in electrode 153 compared to electrodes 166 and 170. Based on the spectra shown in figure 2, it is estimated that electrode 153 contains roughly 85 % magnetite (or possibly wüstite) and 15 % hematite. Samples prepared using $FeCl_3$ and $Fe(acac)_3$ precursors should be expected to contain around 70 % hematite. It should be stressed that these numbers are estimates: an attempt to accurately quantify the relative concentrations of each component through modelling the spectrum of a thin film using a basis set of component spectra is underway. However, it has been suggested that using traditional dispersive spectrometers, the limit of detection of, say, magnetite in a binary mixture of hematite may be as high as 30 %[3]. It is hoped that this could be overcome using a confocal Raman microscope.

Given that the crystallinity and also the structure of the films are expected to be crucial to their performance it is notable that the composition, as determined by Raman spectroscopy can qualitatively follow the photoactivity of the electrodes. For example, figure 4 shows the Raman spectra of two electrodes prepared using a $FeCl_3$ precursor.

Here, the band at 661 cm^{-1} in the Raman spectrum of electrode 71 is more intense than the band at 410 cm^{-1}, which is assigned to hematite. Electrode 71 was found to afford poor photocatalysis, whereas electrode 166 gave good photoactivity. From figure 4, it can be seen that the band at 661 cm^{-1} has less than half the intensity of the hematite band at 411 cm^{-1}. This evidence, along with the photoactivity and composition of the Raman spectra of the $Fe(NO_3)_3$-prepared electrodes indicate

that Raman microscopy is an extremely useful technique for probing the surface structure, furthermore, it is possible to gain qualitative information regarding the performance of the iron oxide films.

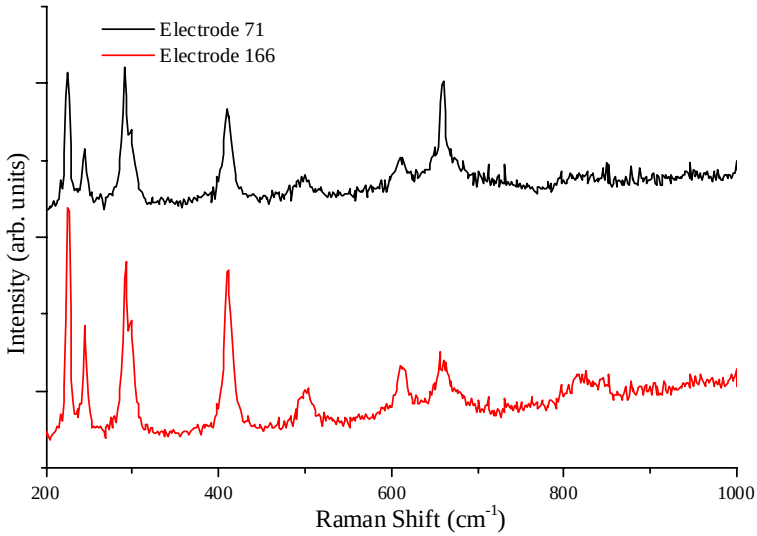

Fig. 4. Raman spectra of two $FeCl_3$-prepared electrodes.

X-ray diffraction (RX)

THE X-RAY DIFFRACTION MEASUREMENTS HAVE BEEN PERFORMED ON A BRAGG-BRENTANO-FOCUSSING, PLANAR GOEBEL-MIRROR DIFFRACTOMETER WITH GRAZING INCIDENCE, USING CR-Kα RADIATION AND PSE DETECTOR.

The intense and sharp peaks observed in fig. 5 (indicated by blue lines) can be attributed to the SnO_2 overlayer on glass, crystallised as cassiterite, syn-SnO_2. The sharpness of these bands reflects high crystallinity of this species. In comparison, the α-hematite present in the film seems partly amorphous, but the presence of a well-crystallised fraction can be observed (indicated by the red lines) upon comparison with the X-ray diffraction pattern of pure hematite. Experiments are ongoing in an attempt to find a more precise correlation between the measured photocurrents and the characteristics of X-ray diffraction patterns observed for our electrodes.

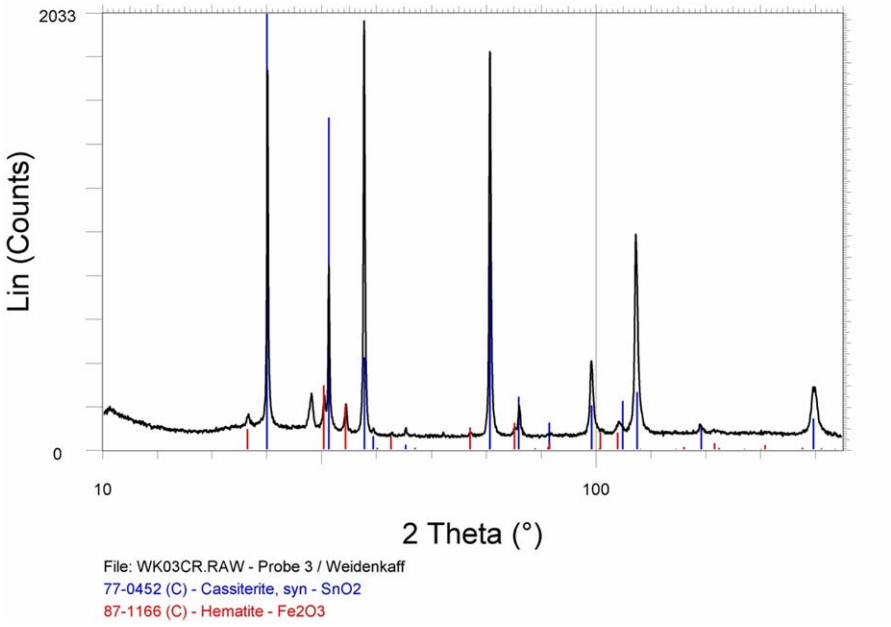

Fig. 5 X-ray diffraction pattern of an iron oxide thin film (type C) deposited on conducting glass (bearing a SnO_2 overlayer)

Triple photoelectrolysis cell.

Due to the presence of a short hole diffusion length in ferric oxide along with its relatively high resistivity, an increase of the film thickness above *ca.* 1 μm leads usually to a decrease in the photocurrents obtained under moderate anodic bias. However, such small film thickness imposes a severe limitation with regard to the portion of visible light absorbed by the semiconductor especially in the 450-550 nm range of wavelengths close to the band edge (under such conditions the penetration depth of incident light exceeds significantly the film thickness). In an attempt to overcome this difficulty, a photoelectrolysis cell has been constructed in which three thin film Fe_2O_3 electrodes were placed one behind another and connected electrically in parallel (*cf.* scheme 1). These electrodes were prepared using ferric acetylacetonate solution (precursor type A) since the corresponding films exhibit superior transparency to the wavelengths longer than 550 nm and are thus compatible with an application in a tandem PEC cell. Fig. 6 shows photocurrent-voltage curves recorded for each electrode separately and for the three electrodes connected together. In particular, the presence of a second electrode results in a significant improvement in the generated photocurrent.

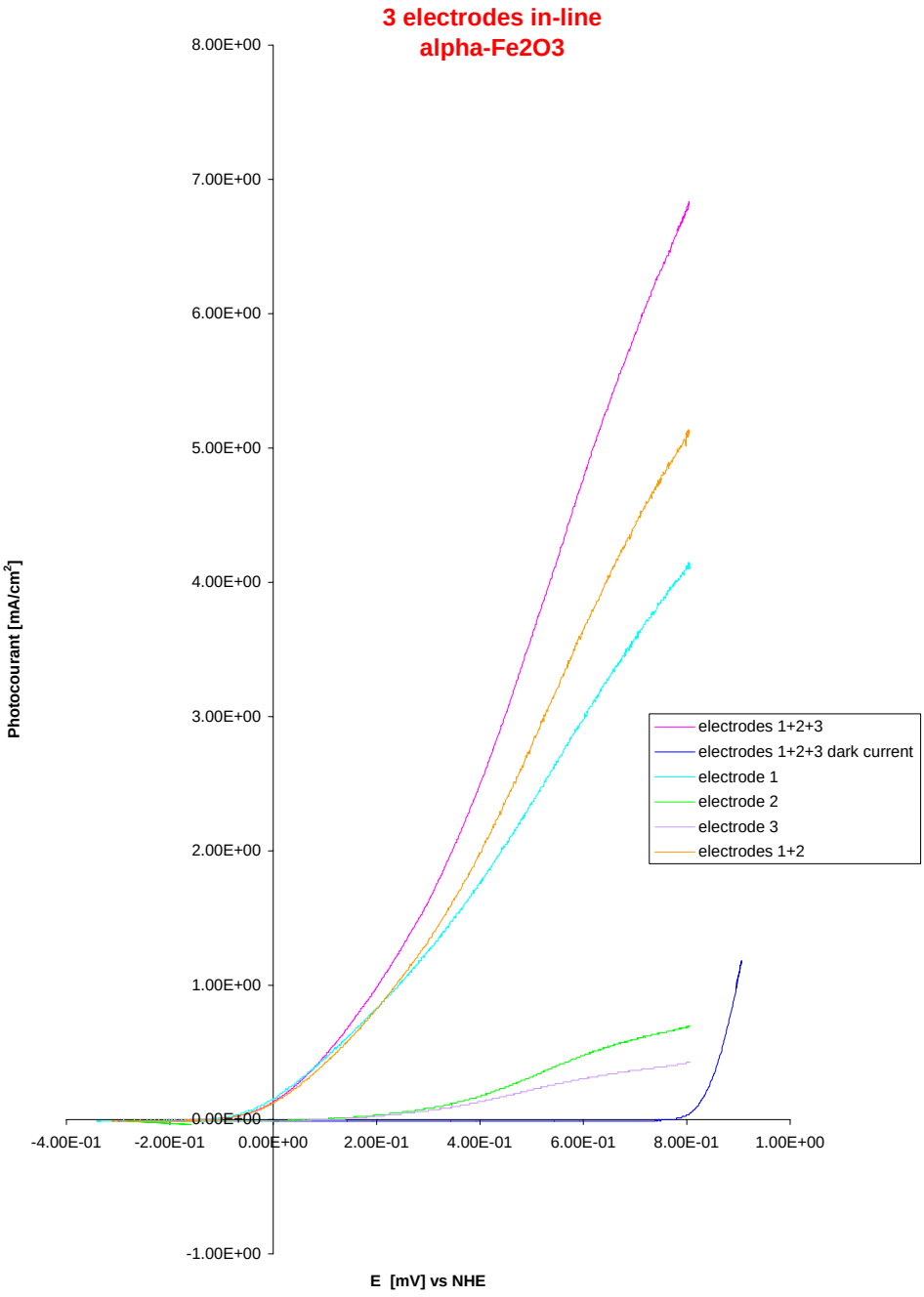

Fig. 6 Photocurrent-voltage curves for a three-photoanodes cell (using undoped electrodes of type A, 6 layers). Electrolyte NaOH 0.1 M, Xe lamp 150 W.

Scaling-up

At this stage of the project, an important objective pursued was the scaling-up of the photoelectrodes towards a size compatible with a tandem photoelectrolytic cell (PEC) demonstration device for water splitting. It is to be mentioned in this connection that studying of engineering solutions and building of demonstration systems are among the key goals of the proposed extension program of The Hydrogen Implementing IEA Agreement Annex-14. Until last summer, the ferric oxide photoelectrodes prepared and tested in our laboratory had the surface area not exceeding 1 cm^2. At the time of writing of the present report, the 10 x 10 cm electrodes are being tested in association with a liquid-junction photovoltaic (TiO_2-dye) cell of a similar size built by Solaronix (Aubonne). This scaling-up has required a reinvestigation of the spray-pyrolysis parameters in order to avoid temperature gradients along the sprayed conducting glass plates and to obtain the Fe_2O_3 films of homogeneous thickness and density. To minimize the ohmic losses along the substrate, the conducting glass plates covered with a series of thin silver lines (spaced *ca.* 1 cm apart) were employed. In a final version, the silver lines were covered with a fritted glass deposit in order to avoid the attack of silver by the sprayed precursor solution.

The 10 x 10 cm photoelectrodes were prepared using our standard $FeCl_3$ alcoholic solution containing 5% of Ti(IV) (added as titanium ethoxide). In fact, the exact control of the spraying temperature is less critical for the latter precursor than in the case of ferric acetylacetonate solution.

3 Collaborations

Collaboration avec le "National Institute of Materials and Chemical Research", groupe du Dr H. Arakawa, à Tsukuba (Japon).

La collaboration s'est également poursuivie avec nos partenaires américains de l'Annexe 14 IEA; soit le Dr John Turner au NREL -National Renewable Energy Laboratory- (Colorado) et avec le Dr Clovis Linkous à Florida Solar Energy Center.

Anke Weidenkaff, Université d'Augsburg (Allemagne)

Dr Georges Yasemides, CERAM (Angleterre)

4 PUBLICATIONS

Crystallographically Oriented Mesoporous WO_3 Films: Synthesis, Characterization, and Applications

Clara Santato, Marek Odziemkowski, Martine Ulmann, and Jan Augustynski
J. Am. Chem. Soc. **2001,** *123,* 10639-10649

Photoelectrochemical Properties of Nanostructured Tungsten Trioxide Films

Clara Santato, Martine Ulmann, and Jan Augustynski
J. Phys. Chem. B **2001,** *105,* 936-940

Enhanced Visible Light Conversion Efficiency Using Nanocrystalline WO_3 Films

Clara Santato, Martine Ulmann, and Jan Augustynski
Adv. Mater. **2001,** *13 (7),* 511-514

5 CITATIONS

(1) De Faria, D. L. A.; Silva, S. V.; De Oliveira, M. T. *J. Raman Spectrosc.* 1997, *28*, 873-878.

(2) Martin, T. P.; Merlin, R.; Huffman, D. R.; Cardona, M. *Solid State Commun.* 1977, *22*, 565-7.

(3) Thibeau, R. J.; Brown, C. W.; Heidersbach, R. H. *Applied Spectroscopy* 1978, *32*, 532-535 .

(4) Mellor, J. W. *A Comprehensive Treatise on Inorganic and Theoretical Chemistry*; Longmans-Green: London, 1956; Vol. XIII.

(5) Cataliotti, R. S.; Compagnini, G.; Crisafulli, C.; Minico, S.; Pignataro, B.; Sassi, P.; Scire, S. *Surface Science* 2001, *494*, 75-82.